Molecular Biology of the Cell
Vol. 8, 607–620, April 1997

The *Chlamydomonas Dhc1* Gene Encodes a Dynein Heavy Chain Subunit Required for Assembly of the I1 Inner Arm Complex

Steven H. Myster,* Julie A. Knott,* Eileen O'Toole,† and Mary E. Porter*‡

*Department of Cell Biology and Neuroanatomy, University of Minnesota Medical School, Minneapolis, Minnesota 55455; and †Department of Molecular, Cellular, and Developmental Biology, University of Colorado at Boulder, Boulder, Colorado 80309-0347

Submitted October 25, 1996; Accepted January 8, 1997
Monitoring Editor: Mary Beckerle

Multiple members of the dynein heavy chain (*Dhc*) gene family have been recovered in several organisms, but the relationships between these sequences and the Dhc isoforms that they encode are largely unknown. To identify *Dhc* loci and determine the specific functions of the individual Dhc isoforms, we have screened a collection of motility mutants generated by insertional mutagenesis in *Chlamydomonas*. In this report, we characterize one strain, *pf9–3*, in which the insertion event was accompanied by a deletion of ~13 kb of genomic DNA within the transcription unit of the *Dhc1* gene. Northern blot analysis confirms that *pf9–3* is a null mutation. Biochemical and structural studies of isolated axonemes demonstrate that the *pf9–3* mutant fails to assemble the I1 inner arm complex, a two-headed dynein isoform composed of two Dhcs (1α and 1β) and three intermediate chains. To determine if the *Dhc1* gene product corresponds to one of the Dhcs of the I1 complex, antibodies were generated against a Dhc1-specific peptide sequence. Immunoblot analysis reveals that the *Dhc1* gene encodes the 1α Dhc subunit. These studies thus, identify the first inner arm *Dhc* locus to be described in any organism and further demonstrate that the 1α Dhc subunit plays an essential role in the assembly of the I1 inner arm complex.

INTRODUCTION

The dynein ATPases are large multisubunit enzymes that convert the chemical energy derived from binding and hydrolyzing ATP into directed movement along microtubule arrays. Dyneins have been implicated in a wide variety of cellular processes, including vesicle transport, nuclear migration, the spatial organization of membranous organelles, and flagellar motility (reviewed in Holzbauer and Vallee, 1994; Mitchell, 1994; Porter, 1996). Recent studies have used the high degree of sequence conservation within the nucleotide binding site of the dynein motor domain to identify multiple members of the dynein heavy chain (*Dhc*)[1] gene family in *Paramecium*, sea urchin, *Drosophila*, rat, and *Chlamydomonas* (Asai *et al.*, 1994; Gibbons *et al.*, 1994; Rasmusson *et al.*, 1994; Tanaka *et al.*, 1995; Andrews *et al.*, 1996; Porter *et al.*, 1996). Sequence comparisons suggest that the *Dhc* genes can be separated into two major classes: cytoplasmic and axonemal. However, the relationship between the individual genes and the Dhc isoforms they encode is largely unknown (reviewed in Gibbons, 1995), and more recent work has indicated that conclusions about *Dhc* function made on the basis of sequence comparisons or expression profiles may be misleading (Criswell *et al.*, 1996; Vaisberg *et al.*, 1996).

‡ Corresponding author: Department of Cell Biology and Neuroanatomy, 4–135 Jackson Hall, 321 Church Street SE, Minneapolis, MN 55455.

[1] Abbreviations used: cM, centimorgan; Dhc, dynein heavy chain; HMEEN buffer, 30 mM HEPES, pH 7.4, 5 mM $MgSO_4$, 1 mM EGTA, 0.1 mM EDTA, 25 mM NaCl, 1 mM DTT, and 2.5 μg/ml aprotinin, leupeptin, and pepstatin; RFLP, restriction fragment length polymorphism.

Axonemal dynein polypeptides have been studied most extensively in the biflagellate green alga *Chlamydomonas*, where 11 distinct Dhc isoforms have been identified biochemically as components of eight separate dynein complexes. The outer dynein arm is composed of three heavy chains (α, β, and γ), two intermediate chains, and 10 light chains; this complex repeats every 24 nm along the length of the axoneme (reviewed in Mitchell, 1994; Witman *et al.*, 1994). In contrast, the inner dynein arms are more structurally diverse. Two Dhc isoforms, 1α and 1β, in combination with three intermediate chains form the I1 inner arm complex, which is located proximal to the first radial spoke in each 96-nm axonemal repeat (Piperno *et al.*, 1990; Smith and Sale, 1991; Mastronarde *et al.*, 1992; Porter *et al.*, 1992). The remaining six inner arm Dhc isoforms are complexed with various intermediate and light chains to form six single-headed subspecies (Goodenough *et al.*, 1987; Kagami and Kamiya, 1992) that appear to be distributed asymmetrically throughout the axoneme (Piperno and Ramanis, 1991; Kato *et al.*, 1993; Gardner *et al.*, 1994; King *et al.*, 1994).

The study of flagellar mutations has revealed that the outer and inner dynein arms have different functions (Brokaw and Kamiya, 1987). The outer arms provide power to the flagellar beat, and the inner arms are both necessary and sufficient to generate the flagellar waveforms. This functional diversity raises questions as to how the multiple dynein motor complexes are organized and coordinated to produce the different flagellar waveforms. The ability to correlate flagellar mutations with *Dhc* genes and gene products provides a unique opportunity to define the functions of the individual Dhc isoforms. For instance, the three outer arm *Dhc* genes (α, β, and γ) have been linked to three different outer arm loci (*ODA11*, *ODA4/SUP-PF-1*, and *PF28/ODA2/SUP-PF-2*; Sakakibara *et al.*, 1991; 1993; Porter *et al.*, 1994; Wilkerson *et al.*, 1994; Rupp *et al.*, 1996). Phenotypic analysis of the outer arm *Dhc* mutations has further suggested that each isoform has its own unique role in both the assembly of the outer arm complex and the regulation of beat frequency.

Given the number and diversity of inner arm Dhc isoforms, the identification of specific inner arm *Dhc* loci will be critical in understanding the mechanisms that control the different flagellar waveforms. As a first step toward this goal, we have placed eight putative inner arm *Dhc* sequences on the *Chlamydomonas* genetic map by using restriction fragment length polymorphism (RFLP) mapping procedures (Porter *et al.*, 1996). One gene, *Dhc1*, maps within 3 centimorgans (cM) of three closely linked flagellar mutations, *lf2*, *pf9/ida1*, and *ida4*. *lf2* mutations result in abnormally long flagella (McVittie, 1972a,b), whereas *pf9/ida1* and *ida4* represent two different classes of inner dynein arm mutations. *pf9/ida1* mutant axonemes lack the two-headed I1 complex (Kamiya *et al.*, 1991; Porter *et al.*, 1992). *ida4* mutant axonemes lack three single-headed Dhc isoforms that are associated with an actin intermediate chain and a 28-kDa light chain (Kagami and Kamiya, 1992; Mastronarde *et al.*, 1992; LeDizet and Piperno, 1995b). Recent work has shown that the *IDA4* locus corresponds to the structural gene encoding the 28-kDa light chain (LeDizet and Piperno, 1995a). To isolate new mutations that could identify the *Dhc1* locus, we have screened a collection of new motility mutants that were generated by insertional mutagenesis (Tam and Lefebvre, 1993). In our initial screens, we recovered one strain in which ~13 kb of the *Dhc1* gene had been deleted. Further analysis has now shown that the *Dhc1* mutation is a null allele at the *PF9* locus. Characterization of the *pf9–3* mutant phenotype indicates that the *Dhc1* mutation disrupts the assembly of the I1 inner arm complex. Specific antibody probes further reveal that the *Dhc1* gene encodes the 1α Dhc subunit. These studies demonstrate that the 1α Dhc subunit plays an essential role in the assembly and/or targeting of the I1 complex. The recovery of the *pf9–3* mutation, coupled with the characterization of the *Dhc1* transcription unit, also provides the experimental tools with which to identify specific functional domains within the exceptionally large *Dhc* genes.

MATERIALS AND METHODS

Cell Culture and Mutant Strains

Unless noted otherwise, all cells were maintained as vegetatively growing cultures at 21°C on rich medium containing sodium acetate as described by Sager and Granick (1953) and modified by Holmes and Dutcher (1989). All solid media contained Bacto-agar (Difco Laboratories, Detroit, MI) that was washed four times with Milli-Q–filtered water and air dried before use. The medium for large-scale liquid culture was supplemented with additional potassium phosphate as described by Witman (1986). The *arg2* (Eversole, 1956) and *arg7-2* (Loppes, 1969) strains were grown on rich medium with 0.1 the normal concentration of ammonium nitrate and 0.6 mg of arginine/ml of medium. The *nic15* (Hastings *et al.*, 1965) strain was grown on rich medium supplemented with 1 mg/ml yeast extract (Difco Laboratories). The *supcs1–2* (James *et al.*, 1989) strain was grown at 33°C under continuous light. This strain is cold sensitive and will die if grown at 15°C.

Transformation and Screening of Motility Mutants

Three different strains were used as hosts for glass-bead–mediated transformation with a selectable marker as described by Kindle (1990) and Nelson *et al.*, (1994). The strain A54-e18 (*ac17 nit1–1 sr1*) was provided by R. Schnell (University of Minnesota, St. Paul, MN). This strain contains a partial deletion in the nitrate reductase gene and can be transformed with the plasmid pMN56, which contains a wild-type copy of the nitrate reductase gene (Nelson *et al.*, 1994). Six hundred transformants were generated in this laboratory using method 2 as described by Nelson *et al.* (1994). Briefly, A54-e18 cells were grown in liquid SGII medium (Sager and Granick, 1953), concentrated to approximately 1×10^8 cells/ml, and shaken slowly under bright light for 4 h. Approximately 5×10^7 cells in 0.3 ml were combined with 2 μg of linearized pMN56, 0.3 g of glass beads, and

0.1 ml of 20% PEG-8000 and then immediately vortexed for 45 s. The cells were washed with 10 ml of SGII-NO_3 (NH_4NO_3 replaced with 2 mM KNO_3) and plated on SGII-NO_3 medium to select for Nit^+ transformants. After growth on selective medium for 10 d, positive transformants were picked into liquid medium and analyzed for motility defects by phase-contrast light microscopy. Six transformants with aberrant motility phenotypes were chosen for further study. Four additional A54-e18 transformants were provided by J.A.E. Nelson (University of Minnesota).

Twenty transformants with motility defects were obtained from the collection generated by Tam and Lefebvre (1993) using the host strain 5D (*nit1–305, cw15*), which has a point mutation in the nitrate reductase gene (Sosa *et al.*, 1978). These mutants were generated by transformation with the pMN24 plasmid (Fernandez *et al.*, 1989), which contains the nitrate reductase gene within a 14.5-kb insert of *Chlamydomonas* genomic DNA.

Twelve independent transformed cell lines with motility defects were provided by S.K. Dutcher (University of Colorado, Boulder, CO; King and Dutcher, unpublished data). These mutants were collected after transformation of an *arg7–2* strain (Loppes, 1969) with the plasmid pARG7.8, which contains a wild-type copy of the arginosuccinate lyase gene (Debuchy *et al.*, 1989).

Genetic Analysis

Genetic analysis was performed using standard techniques (Levine and Ebersold, 1960; Harris, 1989). Dominance and complementation tests were performed by constructing stable diploid cell lines (Ebersold, 1967). The 116 strain with the *Dhc1* mutation was crossed to the cold-sensitive *supcs1–2* strain to generate a *Dhc1 supcs1–2* double mutant. The appropriate diploid cell line was then selected by mating the *Dhc1 supcs1–2* double mutant to a tester strain containing an auxotrophic marker (either *ac17* or *nic15*) and plating the mating mixtures on minimal medium (Harris, 1989). Cells were grown for 10 d under continuous light at 15°C. At least five independently isolated cell lines were examined for each diploid construction, and all diploids were demonstrated to be mating-type minus.

Analysis of Motility Phenotypes

Motility phenotypes were scored by phase-contrast microscopy on a Zeiss Axioskop microscope using a 40× objective and a 10× eyepiece for a final magnification of 400×. Measurements of swimming velocities were made from video recordings (BV-1000 VCR; Mitsubishi, Tokyo, Japan) of live cells by using a C2400 Newvicon camera and Argus 10 video processor (Hamamatsu Photonic Systems, Bridgewater, NJ) calibrated with a stage micrometer.

Isolation of Genomic Clones

A large insert genomic library constructed in λFIX II (Stratagene, La Jolla, CA) using DNA from the wild-type strain *21 gr* was generously provided by R. Schnell (Schnell and Lefebvre, 1993). This library had been previously screened with a 227-bp polymerase chain reaction product corresponding to the *Dhc1* sequence (GenBank accession number U61364), and ~18 kb of genomic DNA in the region surrounding the predicted nucleotide binding site had been recovered (Porter *et al.*, 1996). We rescreened this library with a genomic fragment (p4A3.6) located 5′ of the region encoding the proposed ATP binding site and recovered 14 overlapping clones that span a total of ~35 kb of genomic DNA. Standard methods were used for plating phage, screening by hybridization (Sambrook *et al.*, 1989), and isolating λ DNA (Chisholm, 1989). Positive clones were restriction mapped with the enzymes *Sac*I, *Sal*I, *Xba*I, and *Not*I. The restriction fragments encoding the ATP hydrolytic domain were identified on Southern blots hybridized with a 4.3-kb genomic fragment previously determined to contain this region (see below; Porter *et al.*, 1996). End fragments were identified by hybridization with T3 and T7 primer sequences present in the λFIX II cloning site. One hundred nanograms of the T3 or T7 primer were end labeled with [α-^{32}P]dCTP and terminal deoxynucleotidyl transferase (Life Technologies, Gaithersburg, MD). Prehybridization and hybridization were done in 4× SSPE (720 mM NaCl, 40 mM sodium phosphate, pH 7.7, 4 mM EDTA), 0.1% SDS, and 0.5 mg/ml heparin at 42°C for the T7 primer and 50°C for the T3 primer.

Southern Blot Analysis

Chlamydomonas DNA was isolated as described by Porter *et al.* (1996). Four micrograms of DNA were digested with the appropriate restriction enzyme, size fractionated on 0.8% agarose gels, and transferred to Zetabind nylon membrane (Cuno, Meriden, CT). DNA probes used for hybridization were purified in low melting point agarose (Life Technologies) and radiolabled with [^{32}P]dCTP and random hexamer primers according to the manufacturer's protocol (Prime It II, Stratagene). Prehybridization was carried out in 6× SSPE (1080 mM NaCl, 60 mM $NaPO_4$, pH 7.7, 6 mM EDTA), 0.5% nonfat dry milk, 0.5% SDS, 50 mM Tris-HCl (pH 7.5), and 500 μg/ml sheared denatured salmon sperm DNA for at least 4 h at 65°C. Hybridizations were done overnight at 65°C in the same solution with the addition of 10% dextran sulfate and a reduced concentration of salmon sperm DNA (100 μg/ml).

Northern Blot Analysis

Cells were grown to late logarithmic phase in 250 ml of TAP medium (Gorman and Levine, 1965). Total RNA was isolated using the method of Wilkerson *et al.* (1994) both before and 45 min after deflagellation induced by pH shock. Total RNA (25 μg/lane) was size fractionated on 0.75% agarose-formaldehyde-denaturing gels, transferred to Zetabind nylon membrane, and immobilized to the membrane by UV irradiation at a setting of 20,000 microjoules (Stratalinker II, Stratagene). Hybridization conditions were identical to those used in the Southern blot analysis.

Protein Purification and Ion Exchange Chromatography

Purified dyneins were prepared from large-scale cultures (40 l) of vegetative cells using procedures described by Witman (1986) and King *et al.* (1986), as modified by Gardner *et al.* (1994). Cells were collected using a Pellicon Cell Harvester (Millipore, Bedford, MA) equipped with Durapore filter cassettes. The cells were washed free of debris and cell wall material by two cycles of resuspension and centrifugation in minimal medium, resuspended in 10 mM HEPES (pH 7.4), 1 mM $SrCl_2$, 4% sucrose, 1 mM dithiothreitol (DTT), and deflagellated by pH shock (Witman *et al.*, 1972). The solution of deflagellated cells was then supplemented to 5 mM $MgSO_4$, 1 mM ethylene glycol-bis(β-aminoethyl ether)-*N,N,N′,N′*-tetraacetic acid (EGTA), 0.1 mM EDTA, and 2.5 μg/ml aprotinin, 2.5 μg/ml leupeptin, and 2.5 μg/ml pepstatin and centrifuged at 1000 × *g*. The supernatant containing the flagella was removed and recentrifuged twice with a 20% sucrose cushion to trap any contaminating cell bodies or debris. Clarified flagella were then collected by centrifugation at 35,000 × *g* for 60 min and resuspended in HMEEN buffer (30 mM HEPES, pH 7.4, 5 mM $MgSO_4$, 1 mM EGTA, 0.1 mM EDTA, 25 mM NaCl, 1 mM DTT, and 2.5 μg/ml aprotinin, 2.5 μg/ml leupeptin, 2.5 μg/ml pepstatin). The purified flagella were then stripped of flagellar membranes by extraction in 1% Nonidet P-40 and washed three times to remove the detergent. The final pellet of whole axonemes was then resuspended in HMEEN buffer containing 0.6 M NaCl, 0.1 mM ATP, and 10 μM Taxol for 30 min to extract the dyneins. The dynein-containing supernatant was collected after centrifugation at 30,000 × *g* for 30 min.

Dynein extracts were further fractionated either by sucrose density gradient centrifugation or by ion exchange chromatography. Sucrose density centrifugation was used to isolate I1 inner arm complexes as a 19S particle as described by Porter *et al.* (1992). The

dynein extracts were dialyzed against HMEEN for 2 h, clarified by centrifugation, loaded onto 5–20% sucrose density gradients (13 ml), and centrifuged in a SW41 rotor (Beckman Instruments, Fullerton, CA) for 11 h at 39,000 rpm. Gradients were collected in 20 fractions of 0.6 ml and analyzed by SDS-PAGE. Ion exchange chromatography was also used to separate the dynein isoforms as described by Goodenough *et al.* (1987) with modifications by Kagami and Kamiya (1992) and Gardner *et al.* (1994). Briefly, the dynein extract was diluted in nine volumes of chromatography buffer (20 mM HEPES, pH 7.4, 10 mM NaCl, 5 mM $MgSO_4$, 1 mM DTT, 1 μg/ml leupeptin) and loaded onto a Mono Q HR5/5 analytical anion exchange column (FPLC system, Pharmacia Biotech, Piscataway, NJ) equilibrated with chromatography buffer. The column was washed with buffer containing 100 mM NaCl, and then the protein was eluted with a linear 100–400 mM NaCl gradient applied over 40 ml. Fractions of 0.5 ml were collected and analyzed by SDS-PAGE. All procedures for dynein fractionation were carried out at 4°C.

SDS-PAGE

The dynein heavy chains were resolved by SDS-PAGE on a 3–5% polyacrylamide, 3–8 M urea gradient gel (Kamiya *et al.*, 1991) using the Laemmli (1970) buffer system. For analysis of the intermediate and lower molecular weight polypeptides, a 5–15% polyacrylamide, 0–2.5 M glycerol gradient gel was used. All gels were stained with silver as described by Wray *et al.* (1981).

Electron Microscopy and Image Analysis

Axonemes were prepared for electron microscopy as described in Porter *et al.* (1992). Longitudinal images were selected, digitized, and averaged as described in Mastronarde *et al.* (1992). The criteria for selecting appropriate longitudinal images included the presence of radial spokes and clear images of the outer arms. The images were normalized to the outer dynein arm with a program that scaled the background image intensity to zero and the mean intensity of the region containing the outer arm to one. Averages of individual axonemes were obtained by averaging at least six 96-nm radial spoke repeats. Averages from several axonemes were then combined to obtain a grand average. The methods used to compare differences between two strains are described in detail in Mastronarde *et al.* (1992).

DNA Sequencing and Analysis

Fragments from the large insert genomic clones were subcloned into pBluescript (Stratagene). A 4.2-kb subclone located 5′ of the region encoding the proposed ATP-binding site was selected for further sequence analysis. Sequence information was obtained from both strands by using a series of nested deletions (Erase-a-Base System, Promega, Madison, WI) and Sequenase 2.0 (Amersham, Arlington Heights, IL) following the manufacturer's instructions. The sequence data were assembled with the GCG software package version 8 (Genetics Computer Group, Madison, WI). Potential open reading frames were identified with the GCG program CodonPreference and a codon usage table that was compiled from the coding regions of several different *Chlamydomonas* nuclear sequences (Silflow *et al.*, 1985; Williams *et al.*, 1989; Savereide, 1991; Mitchell and Brown, 1994; Zhang, 1996; Schnell, personal communication). Potential splice donor and acceptor sequences were also identified based on splice junction consensus sequences found in these same *Chlamydomonas* nuclear genes. The predicted amino acid sequence of this region of the *Dhc1* gene was then compared with the outer arm β and γ Dhc sequences (Mitchell and Brown, 1994; Wilkerson *et al.*, 1994) by using the GCG programs BestFit and Pileup.

Antibody Production and Immunoblot Analysis

Alignment of the predicted amino acid sequences of three Dhc isoforms (β, γ, and Dhc1) identified several regions of sequence divergence within the Dhc1 fragment. These regions were then analyzed for potential antigenicity (Jameson and Wolf, 1988) with the MacVector sequence analysis software package (Eastman Kodak, Rochester, NY). The amino acid sequence DGTCVETPEQRGATD was chosen as the site to design a peptide for antibody production. This peptide corresponds to a region of sequence divergence in the alignment between Dhc1 and amino acid residues 979–988 of the β Dhc (Mitchell and Brown, 1994). The peptide was conjugated to keyhole limpet hemocyanin and injected into two rabbits (Research Genetics, Huntsville, AL); both rabbits were given booster injections and bled at 4-wk intervals for a total of 28 wk. The resulting polyclonal antisera were first tested on Western blots of wild-type axonemes and then affinity purified on Western blots of wild-type dynein extracts (Olmsted, 1981).

To affinity purify the Dhc1 antibody, wild-type dynein extracts were separated on 5% polyacrylamide gels containing reduced amounts of bisacrylamide (25T/1C; see Porter and Johnson, 1983), electroblotted to nitrocellulose (Schleicher & Schuell, Keene, NH), and visualized with Ponceau S (Sigma, St. Louis, MO). The region corresponding to the Dhcs was excised and incubated overnight with a 1:100 dilution of immune serum in 1× phosphate-buffered saline (PBS; 0.58 M Na_2HPO_4, 0.017 M $NaH_2PO_4 \cdot H_2O$, 0.68 M NaCl), 5% normal goat serum (Sigma), and 0.05% Tween 20 (polyethylene-sorbitan monolaurate) at 4°C. The strips were rinsed in 1× PBS followed by three 20-min washes in 50 mM Tris-HCl (pH 7.5), 5 mM EDTA, and 150 mM NaCl. Bound antibodies were eluted by incubation with 1 ml of 3 M potassium thiocyanate and 20 mM Tris-HCl (pH 7.5), for 5 min, and then diluted with 9 ml of 1× PBS and 1% normal goat serum. The affinity-purified antibody was concentrated to approximately 0.5 ml with a Centricon-30 filtration system (Amicon, Beverly, MA).

To resolve the multiple Dhc subspecies and determine which subspecies might be recognized by the Dhc1 antibody, duplicate samples of axonemes, high salt extracts, or purified I1 complexes were separated on 5% polyacrylamide (25T/1C) gels and either stained directly with Coomassie brilliant blue-R250 (Sigma) or electroblotted to nitrocellulose and stained with Ponceau S. The membrane was incubated overnight at 4°C with a 1:10 dilution of the affinity-purified antibody in 1× PBS, 5% normal goat serum, and 0.05% Tween 20. Incubation with an alkaline phosphatase-conjugated secondary antibody and detection with 5-bromo-4-chloro-3-indolyl phosphate and nitroblue tetrazolium were performed according to the manufacturer's instructions (Sigma). Absorption experiments were performed to demonstrate that the affinity-purified antibody is specific for the Dhc1 peptide that was used for immunization. Four different amounts of the peptide (0, 10, 100, and 1000 ng) were incubated with 1 ml of affinity-purified antibody for 60 min at 20°C, and the peptide-antibody mixture was then clarified by centrifugation at 14,000 × *g* for 20 min. The resulting supernatant was then used to probe Western blots containing samples of wild-type axonemes with increasing concentrations of peptide. The intensity of the antibody signal decreased with increasing concentrations of peptide and was completely abolished at the 1000 ng/ml peptide.

RESULTS

Identification of a Dhc1 Mutation at the PF9/IDA1 Locus

In a previous study, we used RFLP mapping procedures to place the *Dhc1* gene on the left arm of linkage group *XII/XIII*, within 3 cM of three closely linked flagellar mutations, *pf9/ida1*, *ida4*, and *lf2* (Figure 1; Porter *et al.*, 1996). To distinguish which locus might be the *Dhc1* gene, we screened a collection of motility mutants generated by insertional mutagenesis with

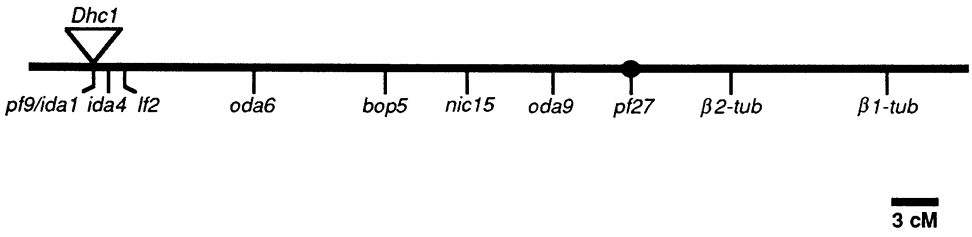

Figure 1. Genetic map location of the *Dhc1* gene. Previous work has shown that the *Dhc1* gene maps to the left arm of linkage group *XII/XIII*, in the vicinity of three flagellar loci, *PF9/IDA1*, *IDA4*, and *LF2* (Porter *et al.*, 1996).

the aim of recovering a *Dhc1* mutation (see MATERIALS AND METHODS and Tam and Lefebvre, 1993). The motility mutants were sorted into three general classes. The first class of mutants displayed gross defects in flagellar assembly. The second class contained cells with two normal length flagella, but the flagella were completely paralyzed. This phenotype is characteristic of mutations in genes encoding central pair or radial spoke structures (Warr *et al.*, 1966; Witman *et al.*, 1978). The final class of transformants could swim forward, but did so with altered waveforms or more slowly than wild type. Based on the motility phenotypes of previously characterized dynein mutations (Brokaw and Kamiya, 1987), we would expect that transformants with mutations in dynein-related genes would fall into this last class. Forty-two transformants with altered waveforms were selected for further study.

To identify potential *Dhc* mutations, DNA samples isolated from the 42 mutants were analyzed on genomic Southern blots. In *Chlamydomonas*, integration of a selectable marker appears to occur randomly throughout the genome and is often accompanied by deletion or rearrangement of the host cell DNA at the site of integration (for review, Tam and Lefebvre, 1993; Gumpel and Purton, 1994). We reasoned that if such an integration event occurred in a *Dhc* gene, we might be able to identify this mutation by hybridization of the Southern blots with probes for the different *Dhc* genes. Figure 2 shows a genomic Southern blot that was loaded with DNA samples from eight motility mutants and hybridized with a probe for the *Dhc1* gene. Most transformants show the wild-type pattern, but the genomic DNA from transformant 116 (Figure 2, lane 3) fails to hybridize with the *Dhc1* probe, suggesting that a portion of the *Dhc1* gene has been deleted in this strain.

To confirm that the motility defect resulted from the insertion of the selectable marker (*ARG7*) into the *Dhc1* gene, we backcrossed transformant 116 to an *arg7* strain with wild-type motility and checked that the motility defect cosegregated with the Arg+ phenotype. Analysis of 22 tetrads and six additional random progeny revealed that all of the slow swimming progeny were able to grow on selective medium, whereas all of the progeny with wild-type motility were unable to grow in the absence of arginine. These results indicate that the Arg+ phenotype is tightly linked to the mutant swimming phenotype (<1.9 cM apart) and suggest that the motility defect in strain 116 is the result of the insertion event.

The *Dhc1* gene is closely linked to three flagellar loci, *LF2*, *PF9* and *IDA4* (Figure 1; Porter *et al.*, 1996). The deletion strain has two normal length flagella, thus the *Dhc1* deletion is unlikely to be a mutation at the *LF2* locus. To test whether the *Dhc1* deletion might represent a new allele at either the *PF9* or *IDA4* locus, we first compared the mutant motility phenotypes. Both inner arm mutants *pf9* and *ida4* swim more slowly than wild type, but the two mutants can be easily distinguished by phase-contrast microscopy because they have different swimming behaviors, and *pf9* cells swim more slowly than *ida4* cells (Kamiya *et al.*, 1991; Porter *et al.*, 1992). The motility phenotype of strain 116 closely resembles that of *pf9*, and measurements of forward swimming velocities confirmed that both strains swim at similar speeds (116 swims at 64.7 ± 10.2 μm/s, whereas *pf9* swims at 63.2 ± 8.7 μm/s). To verify that the motility defect is the result of a new mutation at the *PF9* locus, we performed a series of dominance and complementation tests (Table 1). When either the *pf9–2* or strain 116 is mated to an auxotrophic strain with wild-type motility, the result-

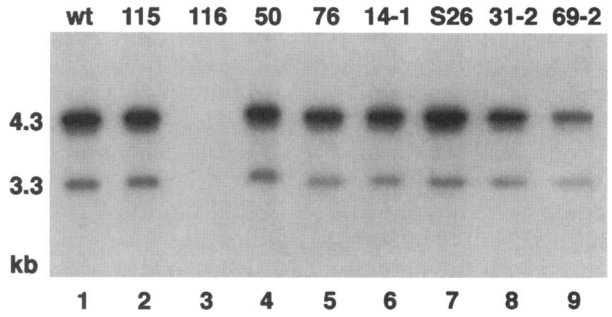

Figure 2. Southern blot analysis of motility mutants generated by insertional mutagenesis. Genomic DNA samples from wild-type (lane 1) and eight motility mutants (lanes 2–9) were digested with *Sac*I, separated on a 0.8% agarose gel, transferred to Zetabind membrane, and hybridized with a 12-kb fragment of the *Dhc1* gene. wt, restriction pattern of a wild-type strain (137c). Genomic DNA from transformant 116 (lane 3) fails to hybridize with the *Dhc1* probe. Stripping and hybridizing the blot with probes for other *Dhc* genes confirmed that equal amounts of DNA were loaded in each lane and that no other *Dhc* polymorphisms were detected in strain 116.

Table 1. Dominance and complementation tests

Diploid genotype	Swimming phenotype	Conclusion
pf9-2 arg2 / *PF9 arg7*	Wild-type	*pf9-2* is recessive.[a]
Dhc1 supcs1 AC17 / *PF9 SUPCS1 ac17*	Wild-type	The *Dhc1* mutation is recessive.
Dhc1 supcs1 NIC15 / *pf9-2 SUPCS1 nic15*	Slow swimming	The *Dhc1* mutation and *pf9-2* are mutant alleles at the same locus.

[a]Porter *et al.* (1992).

ing diploid strains swim with a wild-type motility phenotype, indicating that both mutations are recessive (Porter *et al.*, 1992; and Table 1). However, if *pf9–2* and strain 116 are mated to one another, the two mutations fail to complement, and the resulting diploid strains swim with the slow motility phenotype characteristic of the two parent strains (Table 1). The failure to complement indicates that the two mutations are alleles at the same locus. We therefore refer to strain 116 as *pf9–3*, in keeping with the revised nomenclature for *Chlamydomonas* mutations (Dutcher, 1995).

The pf9–3 Mutation Is a 13-kb Deletion within the Dhc1 Transcription Unit

To determine the extent of the deletion in the *pf9–3* strain, we analyzed genomic DNA isolated from both wild type and *pf9–3* on Southern blots. We first recovered 14 overlapping clones spanning ~35 kb of genomic DNA in the region of the *Dhc1* gene (see MATERIALS AND METHODS). Figure 3A shows a partial restriction map of the *Dhc1* region and the corresponding subclones. Each subclone was then used as a hybridization probe on a genomic Southern. As shown in Figure 3B, probe A identified genomic sequences that are present in both wild type and *pf9–3*, whereas the genomic sequences corresponding to probes B, C, D, and E appear to be missing in *pf9–3*. The restriction fragment corresponding to probe F also appears to be altered in *pf9–3*. This fragment presumably represents one junction where the *ARG7* plasmid inserted into the genomic DNA. Because probe A hybridized to the same size fragment in both wild type and *pf9–3*, we decided to recheck probe B. As shown in Figure 3C, a longer exposure with probe B identified a faint band in the *pf9–3* lane that is shifted relative to wild type. To confirm that the shifted bands in the *pf9–3* lanes correspond to the sites of plasmid insertion, we stripped and rehybridized the Southern blot with a probe for the *ARG7* vector sequences (Figure 3C, blot V). As expected, the vector probe did not hybridize to any restriction fragments in wild-type DNA, but in *pf9–3* DNA, the vector probe hybridized to two restriction fragments that are the same size as the fragments recognized by probes B and F. Figure 3D shows a map of the region containing the *Dhc1* gene in both wild type and *pf9–3*. The insertion of the *ARG7* plasmid was associated with a deletion of approximately 13 kb of genomic DNA in *pf9–3*.

Our Southern blot analysis did not reveal whether the 13-kb deletion in *pf9–3* affects only the *Dhc1* transcription unit or alternatively also disrupts neighboring genes. To determine the size of the *Dhc1* transcription unit, total RNA was isolated from wild-type cells before and after deflagellation and analyzed on Northern blots (Figure 4). Previous work has shown that expression of the *Dhc1* transcript is enhanced by deflagellation (Porter *et al.*, 1996). Figure 4A shows a partial restriction map of the *Dhc1* gene, the subclones used as hybridization probes, and an arrow marking the boundaries of the genomic deletion in *pf9–3*. Probes A3′, B, F, and G (Figure 4B) recognize a single large transcript (>13 kb) that increases in abundance after deflagellation. Because these probes extend beyond the boundaries of the deletion in *pf9–3* and still detect only a single transcript in wild-type RNA, we conclude that the *pf9–3* deletion is contained within the *Dhc1* transcription unit and affects only a single gene.

To determine whether the 13-kb deletion results in the formation of a truncated *Dhc1* transcript that might encode a partially functional Dhc isoform, we also analyzed the expression of the *Dhc1* gene in the *pf9–3* mutant background. Figure 5A shows a Northern blot that was loaded with RNA samples isolated 45 min after deflagellation from one wild-type strain and three different *pf9* mutants, *pf9–3*, *pf9–2*, and *ida1*. Probe A3′ hybridized to a large transcript in the wild-type, *pf9–2*, and *ida1* samples but failed to hybridize to a message of any size in the *pf9–3* RNA. Control experiments confirmed that equal amounts of total RNA were loaded in all lanes (see Figure 5B). These data indicate that *pf9–3* is a null allele of the *Dhc1* gene.

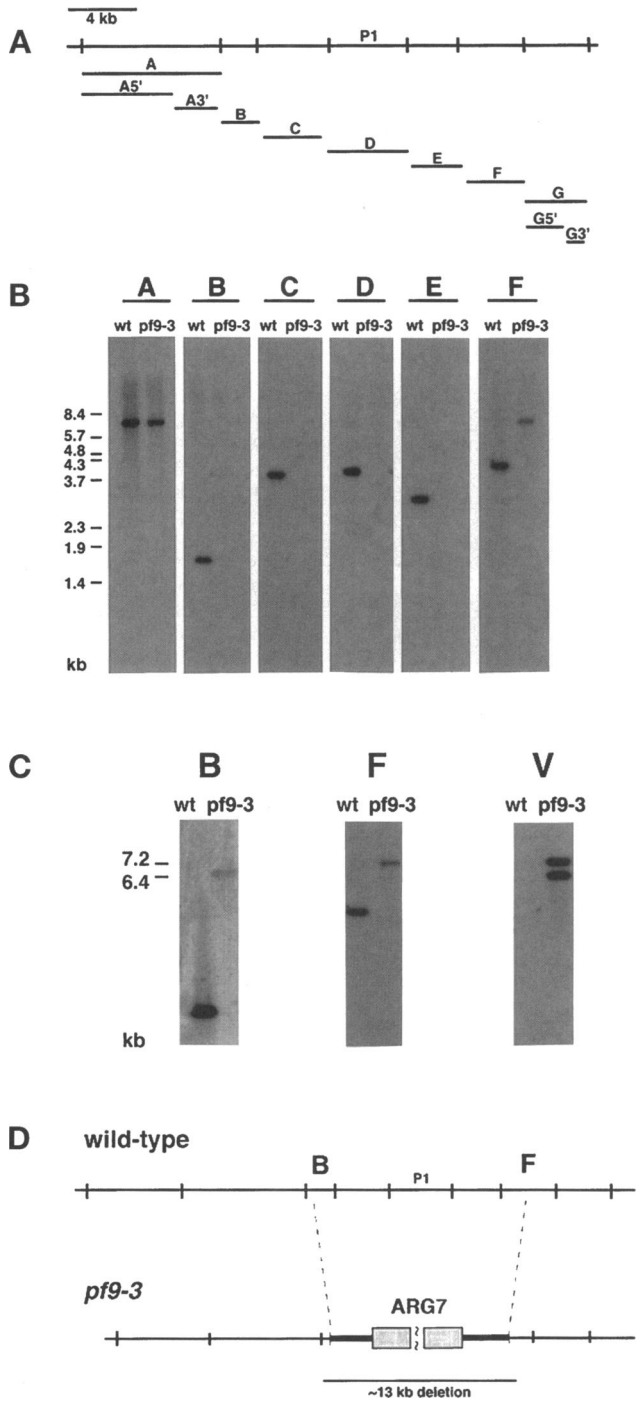

Figure 3. Mapping the deletion in *pf9–3*. (A) The *Sac*I restriction map of wild-type DNA in the region of the *Dhc1* gene. P1 indicates the approximate location of the region encoding the highly conserved Dhc P-loop motif. The positions of probes used to map the deletion in *pf9–3* are also indicated below. (B) Genomic Southern blots of wild-type and *pf9–3* DNA. Duplicate DNA samples from wild type and *pf9–3* were digested with *Sac*I, separated on a 0.8% agarose gel, transferred to Zetabind, and hybridized with fragments of the *Dhc1* gene. (C) Genomic Southern blots identifying restriction fragments containing vector sequences in *pf9–3* DNA. DNA from wild type and *pf9–3* were digested with *Sac*I, separated on a 0.8% agarose gel, and transferred to Zetabind. Probes B and F are *Dhc1* subclones that identify altered restriction fragments in *pf9–3* DNA. The exposure time for probe B was five times longer than was used above in B. Probe V is a 4.6-kb *Bam*HI/*Sal*I vector fragment derived from the plasmid pARG7.8. (D) Schematic diagram comparing the restriction map of the *Dhc1* gene in wild type and *pf9–3*. The insertion of the *ARG7* plasmid in *pf9–3* resulted in a 13-kb deletion of the *Dhc1* gene.

pf9–3 Axonemes Lack the I1 Inner Arm Complex

Dhc mutations within a single locus can display a broad range of phenotypes, ranging from subtle motility defects to the failure to assemble a dynein complex (Sakakibara *et al.*, 1991, 1993; Porter *et al.*, 1994; Rupp *et al.*, 1996). To determine whether the null phenotype of *pf9–3* is similar to that described for other *pf9/ida1* mutations, we characterized *pf9–3* axonemes at both the biochemical and structural levels. Axonemes were isolated from wild-type and *pf9–3* cells and extracted with high salt to release the dynein arms. The high salt extracts were then fractionated by ion-exchange chromatography on a Mono Q column. Figure 6A shows the corresponding FPLC elution profiles. In wild-type extracts, the outer dynein arms elute in two large peaks (γ and α/β), whereas the inner dynein arms elute as seven distinct subspecies (peaks *a–g*; see Kagami and Kamiya, 1992). Peak *f* contains the I1 complex, which typically elutes as a shoulder on the larger peak of the α/β subunit of the outer dynein arm. The elution profile of *pf9–3* appeared to lack peak *f* (Figure 6A). This observation was confirmed by analyzing fractions on polyacrylamide gradient gels. Figure 6B compares the peak fractions from wild type and *pf9–3* separated on 3–5% polyacrylamide gels to resolve the multiple dynein heavy chains. The major heavy chain subspecies in each peak is identified by a dark circle. Peak *f* from the wild-type sample contains the 1α and 1β heavy chains of the I1 complex. These two heavy chains are most easily resolved as they trail into peak *g* and become more separated from the α/β heavy chains of the outer arms. Analysis of the *pf9–3* peak fractions confirmed the presence of all of the Dhcs, except for the two heavy chains of the I1 complex that normally elute in peak *f* (see asterisks). This is most clearly seen in peak *g*, where there is a large gap between the trailing α/β Dhcs of the outer arm and the Dhc isoform associated with inner arm subspecies *g*.

The I1 complex is associated with three intermediate chains, a doublet of 140/138 kDa, and another polypeptide of ~110 kDa (Smith and Sale, 1991; Porter *et al.*, 1992). To determine whether these intermediate chains are missing in *pf9–3* axonemes, samples of peak f from wild type and *pf9–3* were also electrophoresed on a 5–15% polyacrylamide gel (Figure 6C). The asterisks identify the 140/138-kDa doublet and 110-kDa intermediate chains present the wild-type lane. These polypeptides are missing in the *pf9–3* sample. Thus,

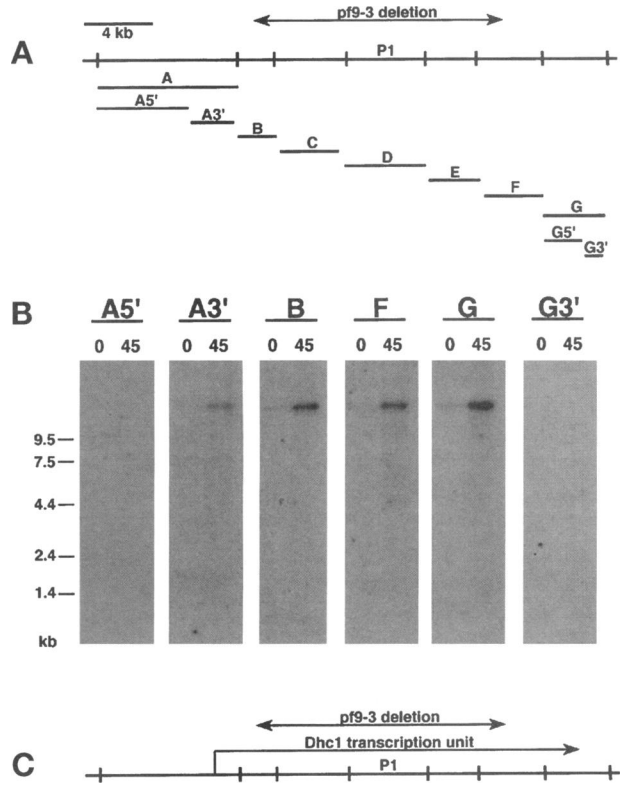

Figure 4. Northern blot analysis of wild-type RNA to identify the boundaries of the *Dhc1* transcription unit. (A) Partial restriction map of the wild-type *Dhc1* gene and subclones used as probes in the Northern blot analysis. The region deleted in the *pf9–3* strain is also indicated. (B) Northern blots of wild-type RNA isolated before (lanes 0) and 45 min after (lanes 45) deflagellation. Parallel samples of 25 μg of total wild-type RNA were separated on 0.75% formaldehyde-agarose gels, transferred to Zetabind, and hybridized with *Dhc1* subclones spanning 30 kb of genomic DNA. A single large transcript that increases in abundance after deflagellation is recognized by probes A3′, B, F, and G but fails to hybridize with probes A5′ and G3′. The *Dhc1* transcription unit therefore spans ~24 kb of genomic DNA, from probe A3′ to probe G. These two probes are located both upstream and downstream of the region deleted in *pf9–3*. (C) Partial restriction map of the *Dhc1* gene. The region deleted in *pf9–3* is shown in relation to the boundaries of the *Dhc1* transcription unit.

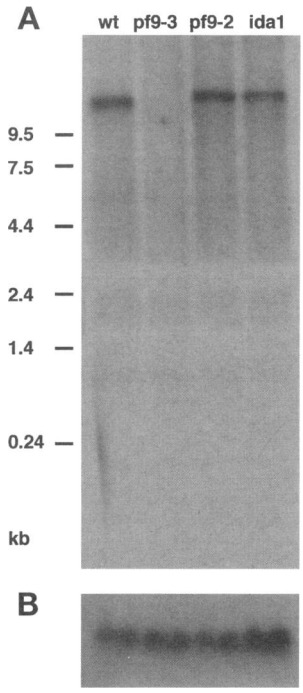

Figure 5. Northern blot analysis of three *Dhc1* mutations. (A) Northern blot of total RNA isolated from wild-type and three different *pf9* mutants. Total RNA was isolated from wild-type, *pf9–3*, *pf9–2*, and *ida1* cells 45 min after deflagellation. RNA, 25 μg from each sample, was separated on a 0.75% formaldehyde-agarose gel, transferred to Zetabind, and hybridized with the A3′ subclone of the *Dhc1* gene. This probe is located within the 5′ end of the *Dhc1* transcription unit and upstream of the region deleted in *pf9–3* (see Figure 4, A and B). The A3′ subclone recognizes the *Dhc1* transcript in RNA isolated from wild type, *pf9–2*, and *ida1*, but no transcript is detected in the *pf9–3* sample. (B) Control blots hybridized with a probe for the *CRY1* gene, which encodes the ribosomal protein subunit S14 (Nelson *et al.*, 1994).

all of the polypeptides associated with the I1 complex fail to assemble into *pf9–3* axonemes.

The inner arm dyneins are a complex group of structures that repeat every 96 nm in register with the radial spokes (Muto *et al.*, 1991; Mastronarde *et al.*, 1992). The I1 complex is the trilobed structure located proximal to the first radial spoke in each 96-nm repeat (Piperno *et al.*, 1990; Mastronarde *et al.*, 1992). To confirm that the structure corresponding to the I1 complex is missing in *pf9–3*, we compared longitudinal views of axonemes from wild type, *pf9*-3, and *pf9–2* by using the image averaging procedures developed by Mastronarde *et al.* (1992). Longitudinal images that contained several axoneme repeats were averaged, and the averages from several axonemes were then combined to obtain a grand average for each sample. The image of the grand average from wild-type axonemes is shown in Figure 7a, and the diagram of the corresponding densities present in the 96-nm repeat is shown in Figure 7b. Figure 7c shows the grand average of longitudinal views of *pf9–3* axonemes. A large gap proximal to the first radial spoke is clearly evident. An analysis of variance between *pf9–3* and wild type confirms that the only significant difference between the two strains is in the densities that make up the I1 complex (Figure 7d). Comparison of *pf9–3* with another *pf9* mutant (*pf9–2*) shows that both strains lack the same structure (see Figure 7, c, e, and f). These images demonstrate that the null phenotype of the *Dhc1* gene is the failure to assemble the I1 complex into the flagellar axoneme.

The 1α Dhc Subunit Is the Protein Product of the Dhc1 Gene

To identify the *Dhc1* gene product and determine its role in the assembly of the I1 complex, we generated a Dhc1 sequence-specific antibody. Previous comparisons of Dhc sequences have shown that the N-terminal third of the Dhc is the most highly variable region (reviewed in Gibbons, 1995). The predicted amino acid sequence of this region was, therefore, compared with the β and γ heavy chains of the outer arm, and several regions of sequence divergence were identified. The peptide DGTCVETPEQRGATD was chosen as a test antigen based on sequence divergence and a favorable antigenicity profile (see MATERIALS AND METH-

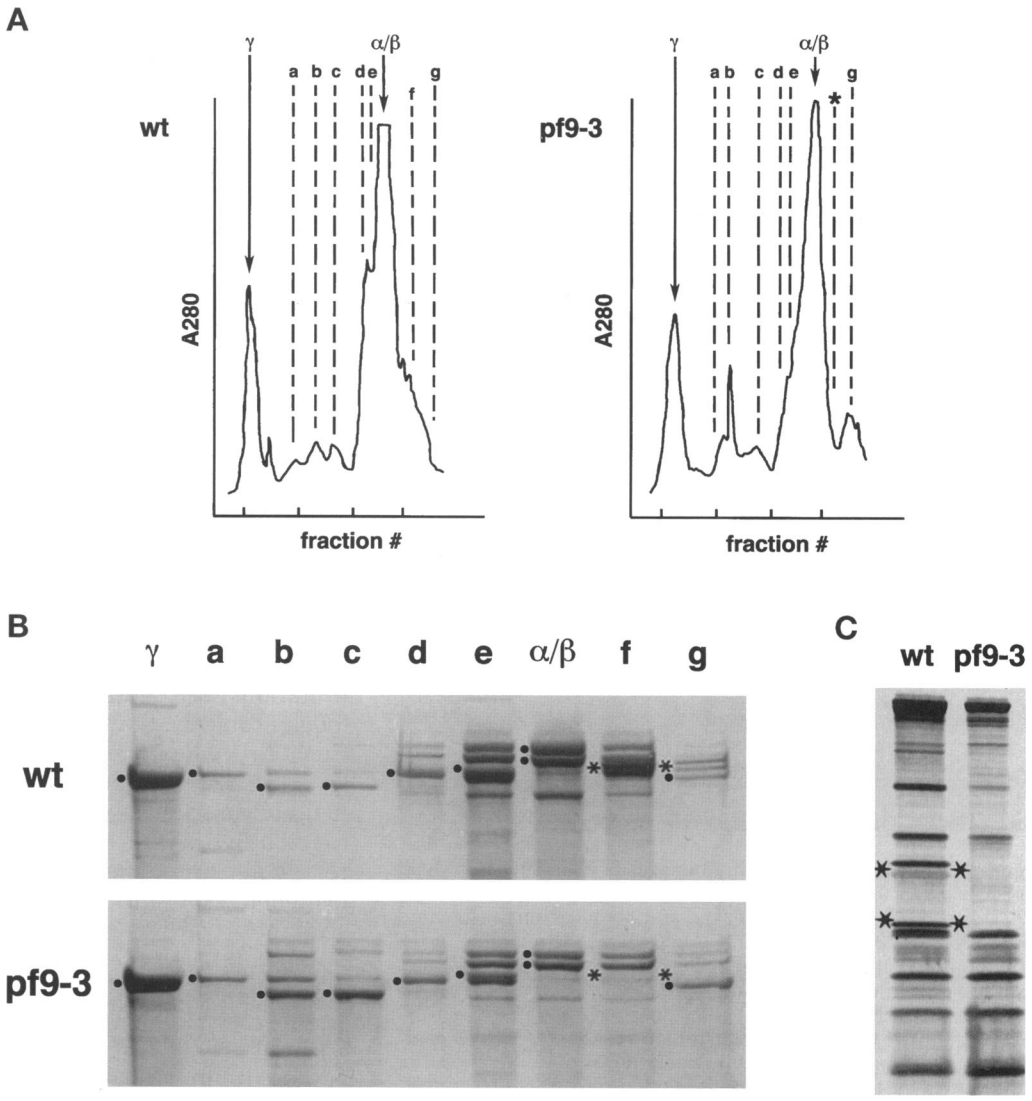

Figure 6. FPLC fractionation of dynein extracts from wild-type and *pf9–3* axonemes. (A) Elution profiles of wild-type and *pf9–3* extracts. Peak fractions containing dynein subspecies are indicated as α/β and γ for the outer arms and as *a–g* for the inner arms. The asterisk denotes the missing peak *f* in the *pf9–3* profile. (B) SDS-PAGE analysis of Dhc isoforms in wild-type and *pf9–3* extracts. Samples of each peak fraction from the wild-type and *pf9–3* profiles were separated on 3–5% polyacrylamide gradient gels containing 3–8 M urea. The major heavy chain isoforms in each peak are denoted by the solid circles. Peak *f* in *pf9–3* lacks the 1α and the 1β heavy chains (see asterisks). (C) Analysis of dynein intermediate chain isoforms in wild type and *pf9–3*. Samples of peak fraction *f* from wild type and *pf9–3* were separated on a 5–15% polyacrylamide gradient gel. The doublet at 140 kDa/138 kDa and the 110-kDa intermediate chain associated with the I1 inner arm complex are indicated by asterisks in the wild-type sample. As noted previously, the 138-kDa polypeptide stains anomalously on silver-stained gels (Porter *et al.*, 1992).

ODS). The peptide was conjugated to the carrier protein keyhole limpet hemocyanin and used as an antigen for production of polyclonal antiserum in rabbits. The resulting antiserum was affinity purified with a mixture of wild-type Dhc isoforms and then tested against fractions containing different Dhc subspecies. The results of this analysis are shown in Figure 8.

To test whether the affinity-purified antibody is specific for a Dhc of the I1 complex, we first compared its reactivity against whole axonemes isolated from wild-type, *pf9–3*, and *pf28* strains. Wild-type axonemes contain the full complement of Dhc isoforms, whereas *pf9–3* axonemes lack the 1α and 1β Dhcs of the I1 complex, and *pf28* axonemes lack the α, β, and γ Dhcs of the outer arm. As shown in Figure 8A (lanes 1′, 2′, and 3′), the affinity-purified antibody recognizes a band in the Dhc region of whole axonemes isolated from wild type and *pf28* but fails to recognize a Dhc band in *pf9–3* axonemes. Similar results were seen with high salt extracts of axonemes containing crude dynein fractions (Figure 8B, lanes 4′, 5′, and 6′). These results indicate that the affinity-purified Dhc1 antibody specifically recognizes a Dhc of the I1 complex. To determine whether the Dhc1 antibody recognizes either the 1α or 1β Dhc, we analyzed purified I1 dynein complexes prepared by sucrose density centrifugation of *pf28* high salt extracts. Because *pf28* has no outer arms, the only Dhcs present in the 19S region of a sucrose gradient are the 1α and 1β Dhcs of the I1 complex. These two heavy chains can be clearly separated from one another on a 5% polyacrylamide gel (Figure 8C, lane 7). As shown in the corresponding immunoblot (Figure 8C, lane 7′), only the 1α heavy chain is recognized by the Dhc1 antibody. These results demonstrate that the *Dhc1* gene encodes the 1α Dhc subunit of the I1 complex, and together with the

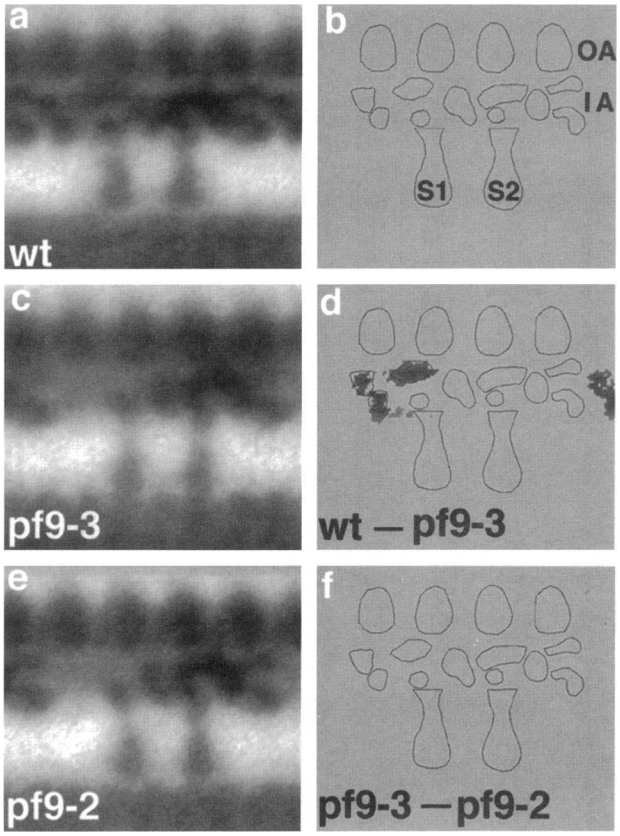

Figure 7. Analysis of longitudinal images of axonemes from wild type (a), *pf9–3* (c), and *pf9–2* (e). Grand averages for wild type, *pf9–3*, and *pf9–2* based on nine, six, and six individual axonemes and 62, 44, and 30 repeating units, respectively. (b) Outline of the individual densities in the 96-nm axonemal repeat. OA indicates positions of four outer dynein arm complexes per 96-nm repeat. IA indicates the structures seen in the inner arm region. S1 and S2 indicate the proximal and distal radial spokes, respectively. (d) Difference plot between wild type and *pf9–3*, with differences not significant at the 0.005 confidence level set to zero. (f) Difference plot between *pf9–3* and *pf9–2*, with differences not significant at the 0.005 confidence level set to zero.

phenotype of the *pf9–3* mutation, also indicate that the 1α Dhc is required for I1 complex assembly.

DISCUSSION

Isolation of Dhc Mutations

The diversity of flagellar waveforms depends on the coordinated activity of multiple dynein motors. At least 15 different *Dhc* genes have been identified in *Chlamydomonas*, three sequences associated with the outer arm (Mitchell and Brown, 1994; Wilkerson *et al.*, 1994) and 12 additional sequences whose expression after deflagellation suggests their axonemal function (Porter *et al.*, 1996; Knott and Porter, unpublished results). Each outer arm *Dhc* gene has been linked to a specific outer arm locus (Sakakibara *et al.*, 1991, 1993; Porter *et al.*, 1994; Wilkerson *et al.*, 1994). Moreover, recent studies of these *Dhc* mutations have provided important insights into the specific roles of each isoform in dynein complex assembly and activity (Sakakibara *et al.*, 1993; Porter *et al.*, 1994; Rupp *et al.*, 1996). However, despite the essential roles played by the inner dynein arms in the generation of the flagellar waveform (Brokaw and Kamiya, 1987), little is known about the specific functions of the individual inner arm Dhcs.

In this study, we provide, the first identification of a *Dhc* gene that encodes an inner arm dynein isoform. Insertional mutagenesis procedures were used to recover a collection of 42 motility mutants with altered flagellar waveforms. DNA samples from the transformants were then analyzed on genomic Southern blots by hybridization with clones corresponding to different *Dhc* genes. With this approach, we identified one transformant in which the insertion of the selectable marker was accompanied by a deletion of ~13 kb of genomic DNA in the region of the *Dhc1* gene (Figures 2 and 3). Recombination analysis confirmed that the motility defect is linked to the selectable marker, and complementation tests demonstrated that the *Dhc1* mutation represents a new allele (*pf9–3*) at the *PF9* locus (Table 1). Southern and Northern blot analyses further revealed that the deletion in *pf9–3* is limited to the *Dhc1* transcription unit and does not extend into neighboring genes (Figures 3 and 4). These results, together with the simplicity of the screen and the relatively large size of *Dhc* genes in *Chlamydomonas* (Mitchell, 1989; and Figure 4), suggest that it should be straightforward to isolate and identify other *Dhc* mutations by using the insertional mutagenesis strategy.

Function of the Dhc1 Gene Product

Although nine different mutant alleles have previously been identified at the *PF9* locus (Hastings *et al.*, 1965; McVittie, 1972a,b; Piperno, 1988; Kamiya *et al.*, 1991; Porter *et al.*, 1992), *pf9–3* is the first allele to be characterized as a *Dhc* mutation. As shown in Figure 4, the deletion in *pf9–3* encompasses more than half of the *Dhc1* gene, including the region that is thought to encode the proposed nucleotide binding sites or P-loops (Knott, Myster, and Porter, unpublished work). A deletion of this size is most likely a null mutation, and consistent with this hypothesis, no *Dhc1* transcript has been detected in *pf9–3* cells (Figure 5). Significantly, the only observable defect in the behavior of *pf9–3* cells is an altered flagellar waveform. These results suggest that the primary function of the *Dhc1* gene product is to contribute to the formation of the flagellar waveform as a component of an inner arm dynein. SDS-PAGE analyses confirm that *pf9–3* mutant axonemes lack the five polypeptides that make up the I1 complex of inner dynein arms (the 1α and 1β Dhcs and three intermediate chains, see Figure 6). Consistent with these polypeptide

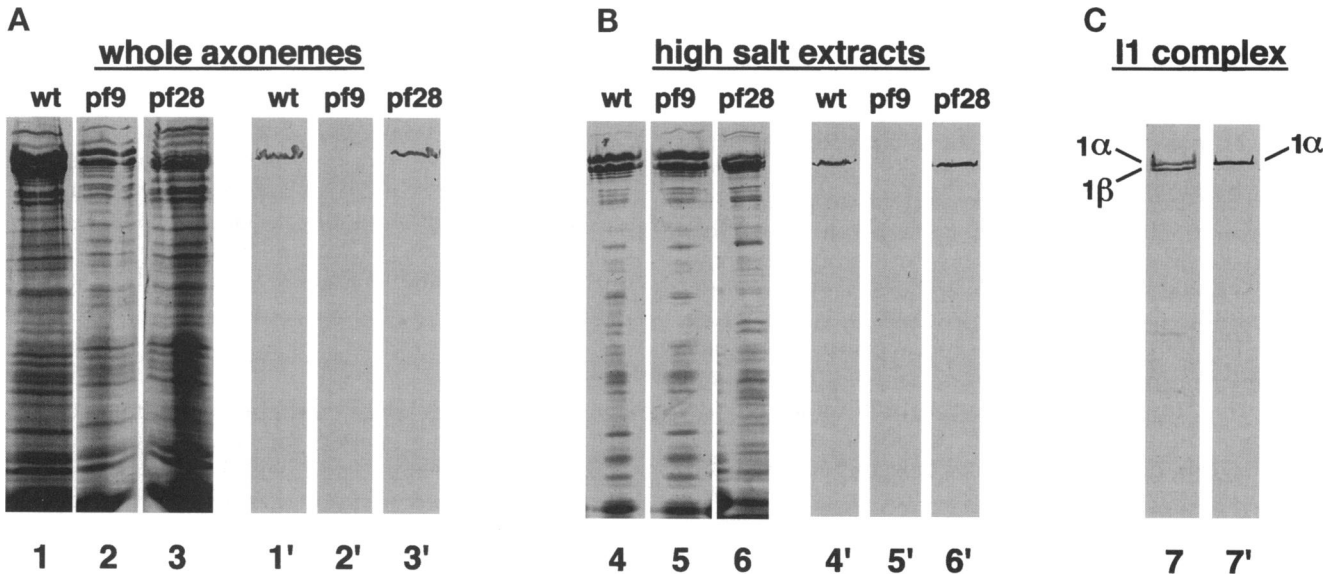

Figure 8. Immunoblot analysis identifies the 1α Dhc as the gene product of the *Dhc1* gene. Duplicate samples were separated on 5% polyacrylamide (25T/1C) gels and either stained with Coomassie blue or electroblotted to nitrocellulose and incubated with the affinity-purified antisera. (A) Gel and corresponding immunoblot of 20 μg of whole axonemes from wild type, *pf9–3*, and *pf28* (lanes 1–3 and 1′–3′). (B) Gel and corresponding immunoblot of 5 μg of crude dynein extracts from wild type, *pf9–3*, and *pf28* (lanes 4–6 and 4′–6′). (C) Gel and corresponding immunoblot of purified I1 complex (lanes 7 and 7′).

defects, images of *pf9–3* axonemes reveal that the tri-lobed structure corresponding to the I1 complex is also missing (Figure 7). Finally, immunoblots probed with a Dhc1 sequence-specific antibody identify the 1α Dhc subunit as the *Dhc1* gene product (Figure 8). Collectively, these results demonstrate that the 1α Dhc plays an essential role in the assembly of the I1 complex. This role is similar to that of the outer arm Dhcs, in which the β and γ Dhcs appear to be required for assembly, but the α Dhc is not (Sakakibara *et al.*, 1991, 1993; Rupp *et al.*, 1996).

Sequence comparisons between members of the *Dhc* gene family have identified homologues of the *Chlamydomonas* Dhc1 sequence in sea urchin (DHC4), *Drosophila* (Dhc98D), and rat (DLP10/axo d) (Gibbons, *et al.*, 1994; Rasmusson *et al.*, 1994; Tanaka *et al.*, 1995; Andrews *et al.*, 1996; Porter *et al.*, 1996). Expression studies in these organisms further demonstrate that the *Dhc1*-related transcripts are most abundant in ciliated cells and tissues (Rasmusson *et al.*, 1994; Andrews *et al.*, 1996) and appear to be up-regulated in response to deciliation (Gibbons *et al.*, 1994; Andrews *et al.*, 1996). Thus, in these organisms, it seems likely that the *Dhc1*-related gene encodes the equivalent of the 1α Dhc subunit of the I1 complex and may thereby contribute to axonemal motility. However, in *Drosophila*, low levels of the *Dhc98D* transcript have also been detected in nonciliated tissues such as embryos and ovaries (Rasmusson *et al.*, 1994). These results raise the possibility that Dhc1-related polypeptides may also function in other forms of microtubule-based motility. Further genetic analysis of the *Drosophila Dhc98D* gene should provide additional insight into this interesting question.

Relationship to Other Dynein Isoforms

Several lines of evidence suggest that the I1 complex is the inner arm isoform that is most similar to both cytoplasmic and outer arm dyneins. First, when viewed by electron microscopy, the isolated I1 complex is a two-headed structure, whereas the other inner arm isoforms appear to be single-headed structures (Goodenough *et al.*, 1987; Smith and Sale, 1991; Kagami and Kamiya, 1992; Mastronarde *et al.*, 1992). Second, phylogenetic analyses of *Dhc* genes indicate that the Dhc1-related sequences form a distinct branch from other putative inner arm Dhc sequences and may be more closely related to the outer arm and cytoplasmic Dhcs (Gibbons, 1995; Tanaka *et al.*, 1995; Porter *et al.*, 1996). Third, preliminary sequence analysis of one of the I1 intermediate chains reveals that it shares regions of homology with both outer arm and cytoplasmic dynein intermediate chains (Yang and Sale, personal communication). Further study of the I1 Dhcs should, therefore, provide insights into the location of conserved domains that are involved in both the assembly of dimeric dynein motors and their targeting to the appropriate cellular cargoes. The relative simplicity of the I1 complex should also be an advantage in experimental efforts to address these questions.

Relationship to Other Inner Arm Loci

Previous work has identified several mutant loci that affect the assembly of inner arm isoforms, but *PF9* is the first locus to be identified as the structural gene for an inner arm Dhc. To understand how the 1α Dhc interacts with other axoneme components to assemble and target the I1 complex, it will be important to identify and characterize the gene products of the other I1 inner arm loci. Thus far, mutations that disrupt I1 complex assembly have been recovered in four other complementation groups; *IDA2* and *IDA3* (Kamiya *et al.*, 1991) and two new loci recently identified by insertional mutagenesis, *IDA7* and *IDA8* (Perrone and Porter, unpublished results). Preliminary RFLP mapping suggests that the *IDA2* locus may correspond to another *Dhc* gene and possibly encode the second Dhc of the I1 complex (Porter *et al.*, 1996; Myster and Porter, unpublished results). By analogy with outer arm mutant loci (Mitchell and Kang, 1991; Takada and Kamiya, 1994; Wilkerson *et al.*, 1995), the remaining I1 loci may encode dynein intermediate chains or accessory proteins involved in the attachment of the I1 complex to the proper site on outer doublet microtubules. In this regard, further analysis of the new I1 mutations generated by insertional mutagenesis should be particularly useful. These mutations can be screened with the currently available clones for dynein-related sequences, or alternatively, the affected genes can be cloned by using standard molecular biological techniques to recover genomic DNA adjacent to the site of plasmid insertion. Both of these strategies have been used to identify and clone flagellar loci in *Chlamydomonas* (Tam and Lefebvre, 1993; Smith and Lefebvre, 1996; this study; Perrone, Yang, Sale, and Porter, unpublished results).

Role of the I1 Complex in Flagellar Motility

Several studies have indicated that the I1 complex is a major target of regulatory mechanisms that control the flagellar waveform. For instance, the *pf9–2* mutation was originally isolated as an extragenic suppressor that could restore partial motility to a paralyzed central pair defective strain (Porter *et al.*, 1992). These observations implicated the I1 complex as an important component of the signaling pathway between the central pair/radial spoke complex and the dynein arms. In vitro pharmacological studies have also demonstrated that microtubule sliding velocities are dramatically reduced in radial spoke/central pair defective axonemes (Smith and Sale, 1992) but that these decreases in sliding velocities can be overcome by treatment of radial spoke/central pair defective axonemes with protein kinase inhibitors (Howard *et al.*, 1994). However, if the mutant axonemes also lack the I1 complex, treatment with protein kinase inhibitors has no effect on axoneme sliding velocities (Habermacher and Sale, 1995). These results suggested that the phosphoprotein, which is the physiologically relevant target of the kinase/phosphatase pathway might be a component of the I1 complex. More recent studies have now identified one of the I1 intermediate chains as a regulatory subunit (Habermacher and Sale, 1997; King and Dutcher, 1997). However, additional work is still needed to understand how modification of a dynein intermediate chain regulates the motor activity of its associated Dhcs. The ability to introduce modified Dhc constructs should provide important information about the nature of these subunit interactions.

Future Studies

The isolation of the *pf9–3* mutation and the discovery that the *Dhc1* gene encodes the 1α Dhc subunit also provide an important experimental foundation for future studies aimed at understanding how a dynein motor complex is assembled and targeted to its proper location within the axoneme. For instance, the 1α Dhc may bind directly to the outer doublet microtubule and thereby promote the assembly of other components of the I1 complex. Alternatively, some portion of the 1α Dhc may be necessary to assemble the I1 complex within the cell body. The complex could then be targeted to its location on the outer doublet by other associated polypeptides. We are currently introducing wild-type and modified constructs of the *Dhc1* gene into the *pf9–3* null mutant background to identify the domains of the Dhc that contribute to dynein complex formation and assembly into the flagellar axoneme. These experiments should also provide important insights into the location of conserved domains that perform similar functions in other dynein isoforms.

ACKNOWLEDGMENTS

We thank S.K. Dutcher, J.A.E. Nelson, and L.W. Tam for generously providing several motility mutants. Many thanks also to members of the laboratories of P.A. Lefebvre and C.D. Silflow (University of Minnesota) for helpful advice throughout this work. T.S. Hays, C.A. Perrone, and J. Rupp also provided constructive comments on the manuscript. Parts of this work were completed by S.H.M. in partial fulfillment of the requirements for the degree of Doctor of Philosophy (University of Minnesota). Support for this work was provided by grants from the National Science Foundation (MCB-9305217) and the March of Dimes (FY94–0612) to M.E.P. S.H.M. was also supported in part by a research training grant (BIR-9113444) for Interdisciplinary Studies on the Cytoskeleton from the National Science Foundation. The Laboratory for 3-Dimensional Microscopy (University of Colorado) was supported by a National Institutes of Health Biotechnology Resource grant (RR00592) to J.R. McIntosh, Director.

REFERENCES

Andrews, K.L., Nettesheim, P., Asai, D.J., and Ostrowski, L.E. (1996). Identification of seven rat axonemal dynein heavy chain genes: expression during ciliated cell differentiation. Mol. Biol. Cell 7, 71–79.

Asai, D.J., Beckwith, S.M., Kandl, K.A., Keating, H.H., Tjandra, H., and Forney, J.D. (1994). The dynein genes of *Paramecium tetraurelia*.

Sequences adjacent to the catalytic P-loop identify cytoplasmic and axonemal heavy chain isoforms. J. Cell Sci. *107*, 839–847.

Brokaw, C.J., and Kamiya, R. (1987). Bending patterns of *Chlamydomonas* flagella IV. Mutants with defects in inner and outer dynein arms indicate differences in dynein arm function. Cell Motil. Cytoskeleton *8*, 68–75.

Chisholm, D. (1989). A convenient procedure for obtaining DNA from bacteriophage lambda. Biotechniques *7*, 21–23.

Criswell, P.S., Ostrowski, L.E., and Asai, D.J. (1996). A novel cytoplasmic dynein heavy chain: expression of DHC1b in mammalian ciliated epithelial cells. J. Cell Sci. *109*, 1891–1898.

Debuchy, R., Purton, S., and Rochaix, J.-D. (1989). The arginosuccinate lyase gene of *Chlamydomonas reinhardtii*: an important tool for nuclear transformation and for correlating the genetic and molecular maps of the *ARG7* locus. EMBO J. *8*, 2803–2809.

Dutcher, S.K. (1995). Genetic nomenclature guide. Trends Genet. *3* (suppl.), 16–18.

Ebersold, W.T. (1967). *Chlamydomonas reinhardti*: heterozygous diploid strains. Science *57*, 446–449.

Eversole, R.A. (1956). Biochemical mutants of *Chlamydomonas reinhardi*. J. Bot. *43*, 404–407.

Fernandez, E., Schnell, R., Ranum, L.P.W., Hussey, S.C., Silflow, C.D., and Lefebvre, P.A. (1989). Isolation and characterization of the nitrate reductase structural gene of *Chlamydomonas reinhardtii*. Proc. Natl. Acad. Sci. USA *86*, 6449–6453.

Gardner, L.C., O'Toole, E., Perrone, C.A., Giddings, T., and Porter, M.E. (1994). Components of a "dynein regulatory complex" are located at the junction between the radial spokes and the dynein arms in *Chlamydomonas* flagella. J. Cell Biol. *127*, 1311–1325.

Gibbons, I.R. (1995). Dynein family of motor proteins: present status and future questions. Cell Motil. Cytoskeleton *32*, 136–144.

Gibbons, B.H., Asai, D.J., Tang, W.J., Y., Hays, T.S., and Gibbons, I.R. (1994). Phylogeny and expression of axonemal and cytoplasmic dynein genes in sea urchins. Mol. Biol. Cell *5*, 57–70.

Goodenough, U.W., Gebhart, B., Mermall, V., Mitchell, D.R., and Heuser, J.E. (1987). High pressure liquid chromatography fractionation of *Chlamydomonas* dynein extracts and characterization of inner arm dynein subunits. J. Mol. Biol. *194*, 481–494.

Gorman, D.S., and Levine, R.P. (1965). Cytochrome f and plastocyanin: their sequence in the photosynthetic electron transport chain of *Chlamydomonas reinhardtii*. Proc. Natl. Acad. Sci. USA *54*, 1665–1669.

Gumpel, N.J., and Purton, S. (1994). Playing tag with *Chlamydomonas*. Trends Cell Biol. *4*, 299–301.

Habermacher, G., and Sale, W.S. (1995). Regulation of dynein-driven microtubule sliding by an axonemal kinase and phosphatase in *Chlamydomonas* flagella. Cell Motil. Cytoskeleton *32*, 106–109.

Habermacher, G., and Sale, W.S. (1997). Regulation of flagellar dynein by phosphorylation of a 138-kD inner arm dynein intermediate chain. J. Cell Biol. *136*, 167–176.

Harris, E. (1989). The Chlamydomonas Sourcebook, San Diego, CA: Academic Press, 399–446.

Hastings, P.J., Levine, E.E., Cosbey, E., Hudock, M.O., Gillham, N.W., Surzycki, S.J., Loppes, R., and Levine, R.P. (1965). The linkage groups of *Chlamydomonas reinhardi*. Microb. Genet. Bull. B *23*, 17–19.

Holmes, J.A., and Dutcher, S.K. (1989). Cellular asymmetry in *Chlamydomonas reinhardtii*. J. Cell Sci. *94*, 273–285.

Holzbauer, E.L.F., and Vallee, R.B. (1994). Dyneins: molecular structure and cellular function. Annu. Rev. Cell Biol. *10*, 339–372.

Howard, D.R., Habermacher, G., Glass, D.B., Smith, E.F., and Sale, W.S. (1994). Regulation of *Chlamydomonas* flagellar dynein by an axonemal protein kinase. J. Cell Biol. *127*, 1683–1692.

James, S.W., Silflow, C.D., Thompson, M.D., Ranum, L.P.W., and Lefebvre, P.A. (1989). Extragenic suppression and synthetic lethality among *Chlamydomonas reinhardtii* mutants resistant to anti-microtubule drugs. Genetics *122*, 567–577.

Jameson, B.A., and Wolf, H. (1988). The antigenic index: a novel algorithm, for predicting antigenic determinants. Comput. Appl. Biosci. *4*, 181–186.

Kagami, O., and Kamiya, R. (1992). Translocation and rotation of microtubules caused by multiple species of *Chlamydomonas* inner-arm dynein. J. Cell Sci. *103*, 653–664.

Kamiya, R., Kurimoto, E., and Muto, E. (1991). Two types of *Chlamydomonas* flagellar mutants missing different components of inner-arm dynein. J. Cell Biol. *112*, 441–447.

Kato, T., Kagami, O., Yagi, T., and Kamiya, R. (1993). Isolation of two species of *Chlamydomonas reinhardtii* flagellar mutants, *ida5* and *ida6*, that lack a newly identified heavy chain of the inner dynein arm. Cell Struct. Funct. *18*, 371–377.

Kindle, K.L. (1990). High frequency nuclear transformation of *Chlamydomonas reinhardtii*. Proc. Natl. Acad. Sci. USA *87*, 1228–1232.

King, S.J., and Dutcher, S.K. (1977). Phosphoregulation of an inner dynein arm complex in *Chlamydomonas reinhardtii* is altered in phototactic mutant strains. J. Cell Biol. *136*, 177–191.

King, S.J., Inwood, W.B., O'Toole, E.T., Power, J., and Dutcher, S.K. (1994). The *bop2–1* mutation reveals radial asymmetry in the inner dynein arm region of *Chlamydomonas reinhardtii*. J. Cell Biol. *126*, 1255–1266.

King, S.M., Otter, T., Witman, G.B. (1986). Purification and characterization of *Chlamydomonas* flagellar dyneins. Methods Enzymol. *134*, 291–306.

Laemmli, U.K. (1970). Cleavage of structural proteins during the assembly of the head of bacteriophage T4. Nature *227*, 680–685.

LeDizet, M., and Piperno, G. (1995a). ida4–1, *ida4–2*, and *ida4–3* are intron splicing mutations affecting the locus encoding p28, a light chain of *Chlamydomonas* axonemal inner dynein arms. Mol. Biol. Cell *6*, 713–723.

LeDizet, M., and Piperno, G. (1995b). The light chain p28 associates with a subset of inner dynein arm heavy chains in *Chlamydomonas* axonemes. Mol. Biol. Cell *6*, 697–711.

Levine, R.P., and Ebersold, W.T. (1960). The genetics and cytology of *Chlamydomonas*. Annu. Rev. Microbiol. *14*, 197–216.

Loppes, R. (1969). A new class of arginine-requiring mutants in *Chlamydomonas reinhardi*. Mol. Gen. Genet. *104*, 172–177.

Mastronarde, D.N., O'Toole, E.T., McDonald, K.L., McIntosh, J.R., and Porter, M.E. (1992). Arrangement of inner dynein arms in wild-type and mutant flagella of *Chlamydomonas*. J. Cell Biol. *118*, 1145–1162.

McVittie, A. (1972a). Flagellar mutants of *Chlamydomonas reinhardtii*. J. Gen. Microbiol. *71*, 525–540.

McVittie, A. (1972b). Genetic studies on flagellum mutants of *Chlamydomonas reinhardtii*. Genet. Res. Camb. *19*, 157–164.

Mitchell, D.R. (1989). Molecular analysis of the alpha and beta dynein genes of *Chlamydomonas reinhardtii*. Cell Motil. Cytoskeleton *14*, 435–445.

Mitchell, D.R. (1994). Cell and molecular biology of flagellar dyneins. Int. Rev. Cytol. *155*, 141–175.

Mitchell, D.R., and Brown, K.S. (1994). Sequence analysis of the *Chlamydomonas* α and β dynein heavy chain genes. J. Cell Sci. *107*, 635–644.

Mitchell, D.R., and Kang, Y. (1991). Identification of *oda6* as a *Chlamydomonas* dynein mutant by rescue with the wild-type gene. J. Cell Biol. *113*, 835–842.

Muto, E., Kamiya, R., and Tsukita, S. (1991). Double-rowed organization of inner dynein arms in *Chlamydomonas* flagella revealed by tilt series, thin-section electron microscopy. J. Cell Sci. *99*, 57–66.

Nelson, J.A.E., Savereide, P.B., and Lefebvre, P.A. (1994). The *CRY1* gene in *Chlamydomonas reinhardtii*: structure and use as a dominant selectable marker for nuclear transformation. Mol. Cell. Biol. *14*, 4011–4019.

Olmsted, J.B. (1981). Affinity purification of antibodies from diazotized paper blots of heterogeneous protein samples. J. Biol. Chem. *256*, 11955–11957.

Piperno, G. (1988). Isolation of a sixth dynein subunit adenosine triphosphatase. J. Cell Biol. *106*, 133–140.

Piperno, G., and Ramanis, Z. (1991). The proximal portion of *Chlamydomonas* flagella contains a distinct set of inner dynein arms. J. Cell Biol. *112*, 701–709.

Piperno, G., Ramanis, Z., Smith, E.F., and Sale, W.S. (1990). Three distinct inner dynein arms in *Chlamydomonas* flagella: Molecular composition and location in the axoneme. J. Cell Biol. *110*, 379–389.

Porter, M.E. (1996). Axonemal dyneins: assembly, organization, and regulation. Curr. Opin. Cell Biol. *8*, 10–17.

Porter, M.E., and Johnson, K.A. (1983). Characterization of the ATP sensitive binding of *Tetrahymena* 30 S dynein to bovine brain microtubules. J. Biol. Chem. *258*, 6575–6581.

Porter, M.E., Knott, J.A., Gardner, L.C., Mitchell, D.R., and Dutcher, S.K. (1994). Mutations in the *SUP-PF-1* locus of *Chlamydomonas reinhardtii* identify a regulatory domain in the β-dynein heavy chain. J. Cell Biol. *126*, 1495–1507.

Porter, M.E., Knott, J.A., Myster, S.H., and Farlow, S.J. (1996). The dynein gene family in *Chlamydomonas reinhardtii*. Genetics *144*, 569–585.

Porter, M.E., Power, J., and Dutcher, S.K. (1992). Extragenic suppressors of paralyzed flagellar mutations in *Chlamydomonas reinhardtii* identify loci that alter the inner dynein arms. J. Cell Biol. *118*, 1163–1176.

Rasmusson, K., Serr, M., Gepner, J., Gibbons, I., and Hays, T.S. (1994). A family of dynein genes in *Drosophila melanogaster*. Mol. Biol. Cell *5*, 45–55.

Rupp, G.,O'Toole, E., Gardner, L.C., Mitchell, B.F., and Porter, M.E. (1996). The *sup-pf-2* mutations of *Chlamydomonas* alter the activity of the outer dynein arms by modification of the γ-dynein heavy chain. J. Cell Biol. *135*, 1853–1865.

Sager, R., and Granick, S. (1953). Nutritional studies in *Chlamydomonas reinhardtii*. Ann. N.Y. Acad. Sci. *56*, 831–838.

Sakakibara, H., Mitchell, D.R., and Kamiya, R. (1991). A *Chlamydomonas* outer-arm dynein mutant missing the alpha heavy chain. J. Cell Biol. *113*, 615–622.

Sakakibara, H., Takada, S., King, S.M., Witman, G.B., and Kamiya, R. (1993). A *Chlamydomonas* outer arm dynein mutant with a truncated beta heavy chain. J. Cell. Biol. *122*, 653–661.

Sambrook, J., Fritsch, E.F., and Maniatis, T. (1989). Molecular Cloning: A Laboratory Manual, 2nd ed., Cold Spring Harbor, NY: Cold Spring Harbor Laboratory Press.

Savereide, P.B. (1991). The molecular basis of resistance to the protein synthesis inhibitor cryptopleurine in *Chlamydomonas reinhardtii*. Ph.D. Thesis. St. Paul, MN: University of Minnesota.

Schnell, R.A., and Lefebvre, P.A. (1993). Isolation of the *Chlamydomonas* regulatory gene *NIT2* by transposon tagging. Genetics *134*, 737–747.

Silflow, C.D., Chisholm, R.L., Conner, T.W., and Ranum, L.P.W. (1985). The two alpha-tubulin genes of *Chlamydomonas reinhardtii* code for a slightly different protein. Mol. Cell. Biol. *5*, 2389–2398.

Smith, E.F., and Lefebvre, P.A. (1996). PF16 encodes a protein with armadillo repeats and localizes to a single microtubule of the central apparatus in *Chlamydomonas* flagella. J. Cell Biol. *132*, 359–370.

Smith, E.F., and Sale, W.S. (1991). Microtubule binding and translocation by inner dynein arm subtype I1. Cell Motil. Cytoskeleton *18*, 258–268.

Smith, E.F., and Sale, W.S. (1992). Regulation of dynein-driven microtubule sliding by the radial spokes in flagella. Science *257*, 1557–1559.

Sosa, F.M., Ortega, T., and Barea, J.L. (1978). Mutants from *Chlamydomonas reinhardtii* affected in their nitrate assimilation capability. Plant. Sci. Lett. *11*, 51–58.

Takada, S., and Kamiya, R. (1994). Functional reconstitution of *Chlamydomonas* outer dynein arms from α-β and γ subunits: requirement of a third factor. J. Cell Biol. *131*, 399–409.

Tam, L.W., and Lefebvre, P.A. (1993). Cloning of flagellar genes in *Chlamydomonas reinhardtii* by DNA insertional mutagenesis. Genetics *135*, 375–384.

Tanaka, Y., Zhang, Z., and Hirokawa, N. (1995). Identification and molecular evolution of new dynein-like protein sequences in rat brain. J. Cell Sci. *108*, 1883–1893.

Vaisberg, E.A., Grissom, P.M., and McIntosh, J.R. (1996). Mammalian cells express three distinct dynein heavy chains that are localized to different cytoplasmic organelles. J. Cell Biol. *133*, 831–842.

Warr, J.R., McVittie, A., Randall, J.T., and Hopkins, J.M. (1966). Genetic control of flagellar structure in *Chlamydomonas reinhardtii*. Genet. Res. *7*, 335–351.

Wilkerson, C.G., King, S.M., Koutoulis, A., Pazour, G.J., and Witman, G.B. (1995). The 78,000 M_r intermediate chain of *Chlamydomonas* outer arm dynein is a WD-repeat protein required for arm assembly. J. Cell Biol. *129*, 169–178.

Wilkerson, C.G., King, S.M., and Witman, G.B. (1994). Molecular analysis of the γ heavy chain of *Chlamydomonas* flagellar outer arm dynein. J. Cell Sci. *107*, 497–506.

Williams, B.D., Velleca, M.A., Curry, A.M., and Rosenbaum, J.L. (1989). Molecular cloning and sequence analysis of the *Chlamydomonas* gene coding for radial spoke protein 3: flagellar mutation *pf-14* is an ochre allele. J. Cell Biol. *109*, 235–245.

Witman, G.B. (1986). Isolation of *Chlamydomonas* flagella and flagellar axonemes. Methods Enzymol. *134*, 280–290.

Witman, G.B., Carlson, K., Berliner, J., and Rosenbaum, J.L. (1972). Chlamydomonas flagella 1. Isolation and electrophoretic analysis of microtubules, membranes, matrix, and mastigonemes. J. Cell Biol. *54*, 507–539.

Witman, G.B., Plummer, J., and Sander, G. (1978). *Chlamydomonas* flagellar mutants lacking radial spokes and central tubules. Structure and function of specific axonemal components. J. Cell Biol. *76*, 729–747.

Witman, G.B., Wilkerson, C.G., and King, S.M. (1994). The biochemistry, genetics, and molecular biology of flagellar dynein. In: Microtubules, ed. J.S. Hyams, and C.W. Lloyd, New York: Wiley-Liss, 229–249.

Wray, W., Boulikas, T., Wray, V.P., and Hancock, R. (1981). Silver staining of proteins in polyacrylamide gels. Anal. Biochem. *118*, 197–203.

Zhang, D. (1996). Regulation of nitrate assimilation in *Chlamydomonas reinhardtii*. Ph.D. Thesis. St. Paul, MN: University of Minnesota.